

Environment-dependent interfacial strength using first principles thermodynamics: The example of the Pt-HfO₂ interface

Y. Cardona Quintero,¹ Ganpati Ramanath,² and R. Ramprasad^{1,a)}

¹*Department of Materials Science and Engineering, Institute of Materials Science, University of Connecticut, 97 North Eagleville Road, Storrs, Connecticut 06269, USA*

²*Department of Materials Science and Engineering, Rensselaer Polytechnic Institute, Troy, New York 12180, USA*

(Received 23 July 2013; accepted 6 October 2013; published online 22 October 2013)

A parameter-free, quantitative, first-principles methodology to determine the *environment-dependent* interfacial strength of metal-metal oxide interfaces is presented. This approach uses the notion of the weakest link to identify the most likely cleavage plane, and first principles thermodynamics to calculate the average work of separation as a function of the environment (in this case, temperature and oxygen pressure). The method is applied to the case of the Pt-HfO₂ interface, and it is shown that the computed environment-dependent work of separation is in quantitative agreement with available experimental data. © 2013 AIP Publishing LLC.

[<http://dx.doi.org/10.1063/1.4826528>]

I. INTRODUCTION

Interfaces between metals and metal oxides are ubiquitous, and encountered in several applications including surface protection, catalysis, and electronics.^{1–7} In every such application, the interfacial mechanical strength determines the overall integrity and performance of the system. Nevertheless, the interfacial strength has defied a quantitative and universal understanding, primarily because it is not an intrinsic property of the system, but a result of the interplay between factors such as interfacial composition,⁴ the atomic-level structure at the interface,^{5,6} and the environment (temperature, pressure, and chemical potentials).^{7,8}

On the experimental side, several well known methods are available to quantitatively understand the linkages between such extrinsic factors and interfacial adhesion, also referred as the work of separation (W_{sep}). These include the four-point bending fracture test⁹ and the contact angle measurement.¹⁰ On the computational side, first-principles density functional theory (DFT) computations have been instrumental in determining and understanding W_{sep} for a plethora of important metal-insulator interfaces.^{3–8,11–25} However, a major drawback of past DFT work is that they apply strictly to 0K situations. Since the interface atomic configuration appropriate for a given set of experimental measurement conditions (temperature and pressure) is *a priori* not known, the general practice has been to compute W_{sep} for a variety of different interfacial atomic configurations. As a result, a direct quantitative comparison of the computed quantities with the corresponding experimentally observed W_{sep} is not always possible.

The present work attempts to fill this gap, by providing a parameter-free scheme to determine the pressure- and temperature-dependent W_{sep} via first principles thermodynamics. While this methodology is general, here, it is applied to the specific case of a Pt-HfO₂ interface for which

experimental W_{sep} is available at high temperatures and low pressures.¹⁰ The choice of the Pt-HfO₂ interface was also motivated by the emergence of HfO₂ as a “high-k” dielectric in next generation transistor technology.²⁶ Our scheme proceeds by considering a variety of O concentrations and atomic arrangements at the interface, and relating them to temperature (T) and O pressure (P_{O₂}) using a statistical mechanical treatment.²⁷ W_{sep} is then determined as a function of T and P_{O₂} by performing statistical averaging.^{1,28}

II. METHODS AND MODELS

Our DFT calculations were performed using the Vienna *ab initio* simulation package (VASP) code,²⁹ with the Perdew-Burke-Ernzerhof (PBE) generalized gradient approximation (GGA)³⁰ and the projector-augmented wave (PAW)³¹ approach. A cutoff energy of 400 eV for the plane wave expansion of the wave functions was used and the calculated results were converged such that the atomic forces were smaller than 0.02 eV/Å.

The Pt-HfO₂ interface was constructed as a $(2 \times \sqrt{3})$ Pt(111) slab strained to match a (1×1) monoclinic HfO₂(001) slab, as reported previously.²⁷ The Pt and HfO₂ slabs contained 5 and 6 layers, respectively, and a vacuum thickness of 14 Å. In this system, one layer of Pt contains 4 Pt atoms and one layer of HfO₂ is formed by 2 atoms of Hf and 4 of O. During the relaxation of the Pt-HfO₂ heterostructure, the 2 layers of Pt farthest from the interface were kept fixed, while the remaining Pt and HfO₂ layers were allowed to relax. In order to obtain converged results, a Monkhorst-Pack k-mesh of $5 \times 5 \times 1$ k-points was used and a dipole correction was applied to compensate for the asymmetric nature of the heterostructures.

Different interfacial O concentrations (θ_O) were considered at the Pt-HfO₂ interface, including 0, 0.25, 0.5, 0.75, and 1 O monolayer (ML). In keeping with the stoichiometry of HfO₂, we define a 1 O ML interfacial layer as containing 2 times the number of Hf atoms per layer. These interfacial

^{a)}Electronic mail: rampi@ims.uconn.edu

O concentrations were selected considering the stability at the expected processing or experimental measurement conditions as suggested by the Pt-HfO₂ phase diagram computed previously using first principles thermodynamics.²⁷ Additionally, the HfO₂ free surface was passivated with 0.5 O ML, as this leads to a fully passivated free surface.³²

III. RESULTS AND DISCUSSION

A. The “virtual” tensile test approach

We begin our analysis with the Pt-HfO₂ system for $\theta_{\text{O}} = 0.5$ O ML, which corresponds to a nominally fully passivated HfO₂ portion at the interface. Fig. 1(a) shows the Pt-HfO₂ 0.5 O ML heterostructure subjected to a “virtual” tensile test. During this process, the external layers (3 of Pt and 4 of HfO₂) were fixed to the relaxed Pt-HfO₂ geometry during successive extensions of 0.02 Å, while the middle layers were allowed to relax, as shown in Fig. 1(a). The evolution of the stress with increasing displacement, along with the geometries of the Pt-HfO₂ structures corresponding to different points of the stress-displacement curve are displayed in Fig. 1(b). The stress was computed from the first derivative of the DFT total energy with respect to the displacement (divided by the interfacial area).

The maximum point in the curve represents the maximum strength of the heterostructure with a value of 5.9 GPa at a 6.4% strain. This point corresponds to the onset of interfacial bond breakage. At a strain of 7.4%, all the bonds at the interface are significantly long and the stress presents a value very close to the maximum. After this point, the stress decreases monotonically. The separated portions of the Pt-HfO₂ 0.5 O ML heterostructure is composed of pure Pt and HfO₂ slabs, the latter fully passivated on both sides. The W_{sep} of this structure, obtained from the integral under the stress-strain curve method described above, has a value of 0.43 J/m².

B. The “weakest link” approach

The virtual tensile test is a common intuitive theoretical method used to determine the W_{sep} of metal-metal oxide

heterostructures.^{5,33,34} However, determination of W_{sep} through such a procedure can be computationally expensive. An alternative, less expensive, and equally accurate method involves the computation of W_{sep} for various choices of cleavage planes across a given heterostructure, and identifying the smallest W_{sep} value. This “weakest link” approach has been used widely as well,^{5,14} and is used here in the determination of the W_{sep} for all the Pt-HfO₂ interfaces considered (including the $\theta_{\text{O}} = 0.5$ O ML case discussed above).

Fig. 2 shows the W_{sep} of all the Pt-HfO₂ heterostructures considered, obtained from the “weakest link” approach. The W_{sep} values are displayed for various cleavage planes for each of the five θ_{O} cases considered (0, 0.25, 0.5, 0.75, and 1 O ML), with $W_{\text{sep}}(\theta_{\text{O}})$ defined as

$$W_{\text{sep}}(\theta_{\text{O}}) = \frac{E_{\text{Pt}} + E_{\text{HfO}_2} - E_{\text{Pt}:\theta_{\text{O}}:\text{HfO}_2}}{A}, \quad (1)$$

where E_{Pt} , E_{HfO_2} , and $E_{\text{Pt}:\theta_{\text{O}}:\text{HfO}_2}$ are the energies of the clean Pt slab, the HfO₂ slab and the Pt-HfO₂ system containing θ_{O} O ML at the interface, respectively, and A is the interfacial surface area of the Pt-HfO₂ system. We note that Eq. (1) can also be expressed as

$$W_{\text{sep}}(\theta_{\text{O}}) = \sigma_{\text{Pt}} + \sigma_{\text{HfO}_2} - \gamma_{\theta_{\text{O}}}, \quad (2)$$

where σ_{Pt} and σ_{HfO_2} are the surface energies of the corresponding Pt and HfO₂ surfaces, respectively, and $\gamma_{\theta_{\text{O}}}$ is the Pt-HfO₂ interfacial energy (defined explicitly below in Eq. (3)). The surface energies were not explicitly evaluated in this work. This was not necessary, as the work of separation could be computed using just the DFT total energies as prescribed by Eq. (1).

First, we consider the $\theta_{\text{O}} = 0.5$ O ML case (the same structure studied in the tensile test above). As we can conclude from Fig. 2, the weakest cleavage plane for this case is the one that leads to a pure Pt slab and a stoichiometric, fully passivated HfO₂ slab (with a $W_{\text{sep}} = 0.39$ J/m²). These observations are in close agreement with the virtual tensile test results, indicating that cleavage is favored along a plane that leads to a fully passivated HfO₂ surface. The latter notion

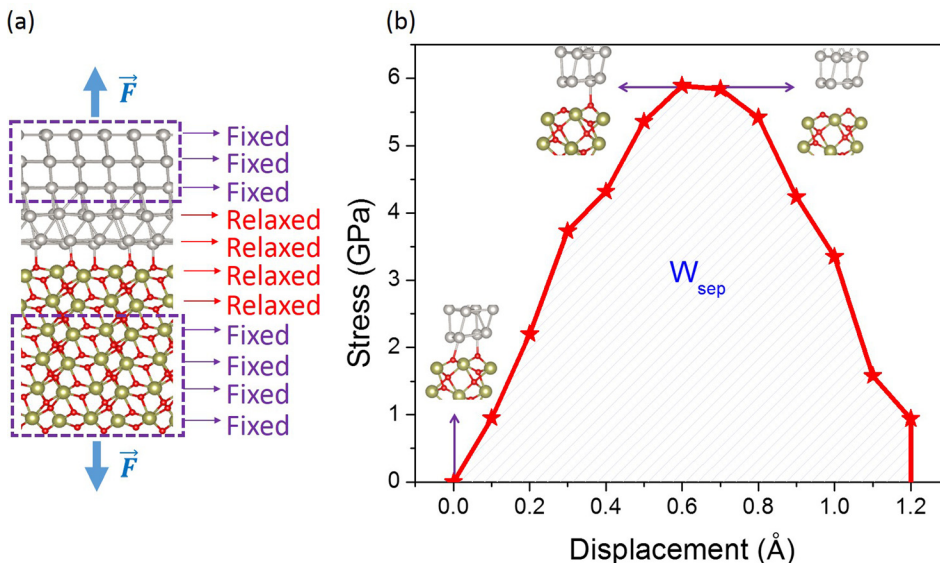


FIG. 1. (a) Pt-HfO₂ heterostructure containing half a monolayer of O at the interface ($\theta = 0.5$ ML) subjected to a tensile test. The fixed and relaxed layers are indicated. (b) Stress-displacement curve of the same Pt-HfO₂ heterostructure. The evolution of the geometry at different values of the strain is indicated as insets. The shaded area corresponds to W_{sep} .

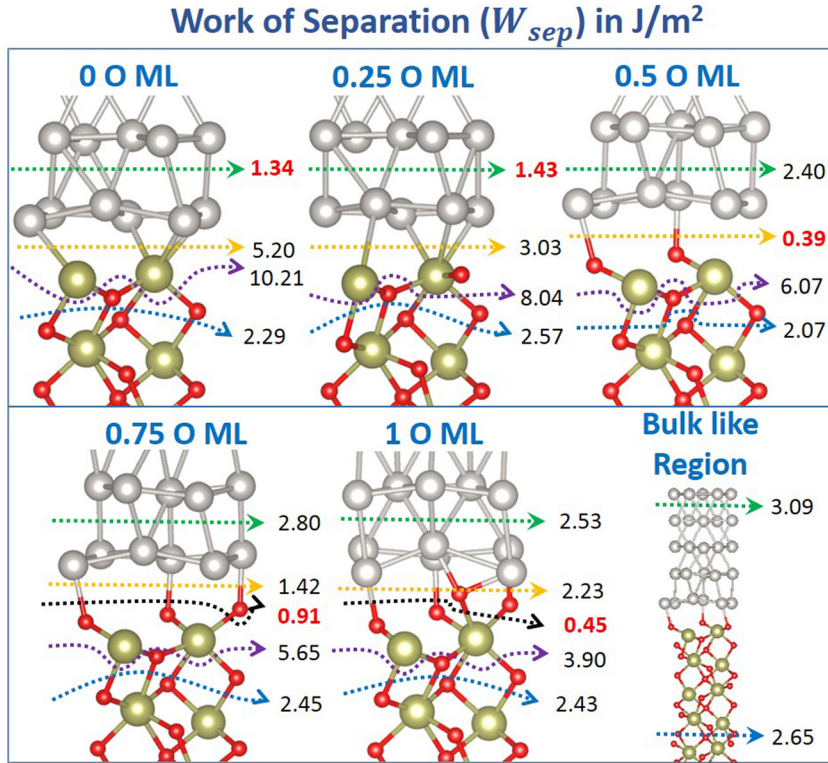


FIG. 2. Work of separation (W_{sep}) in J/m² of Pt-HfO₂ heterostructures for different interfacial O coverages. The dotted lines denote the cleavage planes. Silver, green, and red atoms correspond to Pt, Hf, and O, respectively.

persists as we move on to interfaces containing a higher θ_O , namely, the 0.75 O ML and 1 O ML Pt-HfO₂ heterostructures. In these cases, as can be seen from Fig. 2, the most favored cleavage planes lead to a fully passivated HfO₂ surface (containing $\theta_O = 0.5$ O ML), and the remaining O atoms remain with the cleaved Pt slab. W_{sep} values of 0.91 and 0.45 J/m² are obtained for these “O-rich” interfaces, somewhat higher than the stoichiometric 0.5 O ML Pt-HfO₂ heterostructures. Moving on to the “O-poor” Pt-HfO₂ interfaces, corresponding to $\theta_O = 0$ and 0.25 O ML, the cleavage is preferred such that a pure Pt slab and a sub-stoichiometric HfO₂ slabs with Pt atoms in the surface result. The O-poor interfaces are indeed the strongest ones (with W_{sep} values of 1.43 and 1.34 J/m², respectively), leading to what may perhaps be a general notion as anticipated before,²⁵ namely, that O deficiency at a metal-oxide interface may result in high interfacial strength.

Interestingly, the W_{sep} values of all the 5 heterostructures considered are lower than that of the corresponding pure components. Cleaving a pure Pt system into two portions (leading to two exposed (111) surfaces) requires 3.09 J/m², and the corresponding value for HfO₂ (leading to two passivated (001) surfaces) requires 2.65 J/m², as shown in Fig. 2. Thus, the interfaces are the weakest links regardless of the interfacial O content. A previous DFT study calculated the W_{sep} of the Pt-HfO₂ heterostructure for the same O coverages studied here.⁸ However, only the interfacial plane of each heterostructure was considered.⁸ The values and the tendency obtained here for W_{sep} are consistent with the ones reported in this past work.

C. The environment-dependent W_{sep}

The W_{sep} of the Pt-HfO₂ system has also been determined experimentally by the measurement of the contact

angle,¹⁰ with the measured value being 1.21 J/m² at a temperature of 2073 K and a pressure not higher than 10⁻¹⁰ atm. The DFT computations described thus far indicate that W_{sep} of Pt-HfO₂ interfaces ranges between 0.39 and 1.43 J/m², depending on θ_O at the interface. While the experimental W_{sep} value is indeed bracketed by the corresponding computational estimates, it is desirable to make a more quantitative connection with experiments by taking into account the measurement conditions. A pathway to achieve this is via first principles thermodynamics, which proceeds by the prescription of the interface energy that explicitly depends on T and P_{O_2} .^{1,27,28} γ_{θ_O} of the Pt-HfO₂ system at each θ_O (defined relative to the interfacial energy at $\theta_O = 0.5$ O ML) is given by

$$\gamma_{\theta_O} = [E_{Pt:\theta_O:HfO_2} - E_{Pt:0.5:HfO_2} - (2\theta_O - 1)\mu_{O_2}(T, P_{O_2})]/A, \quad (3)$$

where $\mu_{O_2}(T, P_{O_2})$ is the chemical potential of one O₂ molecule, which can be determined using thermochemical tables or using statistical mechanics, as described elsewhere.^{1,27,28} The T and P_{O_2} dependence of W_{sep} may then be established as follows. In the sense that a statistical distribution of W_{sep} values is expected for each (T, P_{O_2}) conditions, the Pt-HfO₂ stack will display an average W_{sep} value (say, \bar{W}_{sep})

$$\bar{W}_{sep} = \sum W_{sep}(\theta_O) \times \frac{\exp\left(-\frac{\gamma_{\theta_O}(T, P)}{kT}\right)}{\sum \exp\left(-\frac{\gamma_{\theta_O}(T, P)}{kT}\right)}, \quad (4)$$

where k is the Boltzmann constant. In the above equation, the lowest value of W_{sep} among all cleavage planes considered for each choice of θ_O was used as the $W_{sep}(\theta_O)$ value.

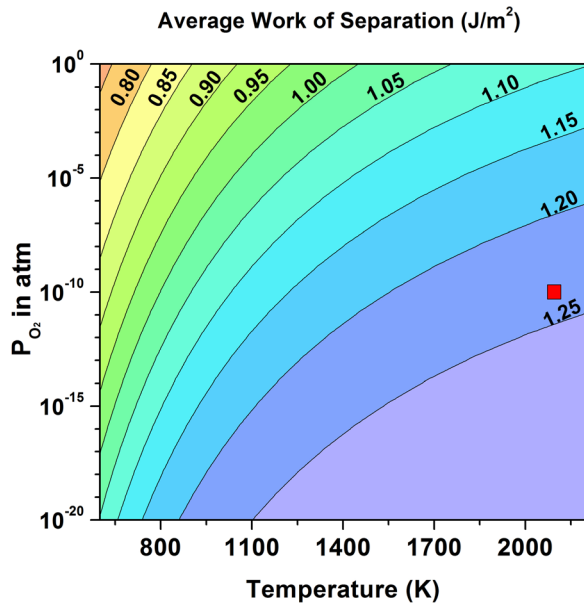


FIG. 3. Average work of separation (\bar{W}_{sep}) as a function of temperature and O pressure of the Pt-HfO₂ interface. The red square represents the experimental conditions at which a 1.21 J/m² value was measured.

Fig. 3 shows \bar{W}_{sep} as function of T and P_{O_2} for the Pt-HfO₂ system. The variation of the \bar{W}_{sep} values can be described in terms of the (T, P_{O_2}) conditions. High T and low P_{O_2} lead to higher \bar{W}_{sep} , while the converse conditions favor low \bar{W}_{sep} values. A comparison of the Pt-HfO₂ phase diagram from first principles thermodynamics²⁷ with Fig. 3 shows that high (low) \bar{W}_{sep} is a consequence of lower (higher) O coverage. This correlation is expected if we consider the behavior of the W_{sep} at different O coverages, described above. Fig. 3 also shows (using a red square) the experimental conditions at which a 1.21 J/m² \bar{W}_{sep} value was measured for the Pt-HfO₂ interface.¹⁰ The computed value under the same measurement conditions of 2073 K and 10⁻¹⁰ atm pressure is 1.25 J/m², in close agreement with the experiments. Experiments also indicate O deficiency at the interface consistent with the discussion above.

IV. CONCLUSIONS

In summary, a parameter-free, predictive methodology to determine the work of separation of a metal-metal oxide interface has been presented. The relevant cleavage plane is identified using the notion of the “weakest link.” The variation of the work of separation with respect to the environment (in this case, temperature and O pressure), which leads to changes in the interfacial O content, has been captured using first principles thermodynamics. The favorable agreement between the computed and experimental results for the Pt-HfO₂ interface under the adopted measurement conditions is indicative of the usefulness of this methodology. Such

approaches may be used to study other interfaces as well, and be effectively used in the rational *ab initio* design of interfaces.

ACKNOWLEDGMENTS

Financial support of this work through a grant from the National Science Foundation (NSF) and computational support through an XSEDE Resource Allocation are gratefully acknowledged.

¹H. Zhu, C. Tang, L. R. C. Fonseca, and R. Ramprasad, *J. Mater. Sci.* **47**, 7399 (2012).

²M. W. Finnis, *J. Phys.: Condens. Matter* **8**, 5811 (1996).

³J. I. Beltran and M. C. Munoz, *Phys. Rev. B* **78**, 245417 (2008).

⁴E. Saiz, R. M. Cannon, and A. P. Tomsia, *Annu. Rev. Mater. Res.* **38**, 197 (2008).

⁵Y. Jiang and J. R. Smith, *J. Mater. Sci.* **44**, 1734 (2009).

⁶S. Kulkova, A. Bakulin, S. Hocker, and S. Schmauder, *IOP Conf. Ser.: Mater. Sci. Eng.* **38**, 012004 (2012).

⁷J. F. Bartolome, J. I. Beltran, C. F. Gutierrez-Gonzalez, C. Pecharroman, M. C. Munoz, and J. S. Moya, *Acta Mater.* **56**, 3358 (2008).

⁸A. V. Gavrikov, A. A. Knizhnik, A. A. Bagatur, B. V. Potapkin, L. R. C. Fonseca, M. W. Stoker, W. Matt, and J. Schaeffer, *J. Appl. Phys.* **101**, 014310 (2007).

⁹D. D. Gandhi, M. Lane, Y. Zhou, A. P. Singh, S. Nayak, U. Tisch, M. Eizenberg, and G. Ramanath, *Nature Lett.* **447**, 299 (2007).

¹⁰A. V. Durov, *Powder Metall. Met. Ceram.* **50**, 552 (2011).

¹¹H. Li, W. Zhang, and J. R. Smith, *Phys. Status Solidi A* **208**, 1166 (2011).

¹²M. Lane, *Annu. Rev. Mater. Res.* **33**, 29 (2003).

¹³A. Trampert, F. Ernst, C. P. Flynn, H. F. Fischmeister, and M. Ruhle, *Acta Metall. Mater.* **40**, S227 (1992).

¹⁴W. Zhang, J. R. Smith, and A. G. Evans, *Acta Mater.* **50**, 3803 (2002).

¹⁵F. Gaudette, S. Suresh, A. G. Evans, G. Dehm, and M. Ruhle, *Acta Mater.* **45**, 3503 (1997).

¹⁶J. Robertson, *Rep. Prog. Phys.* **69**, 327 (2006).

¹⁷J. Robertson, *Solid-State Electron.* **49**, 283 (2005).

¹⁸C. L. Phillips and P. D. Bristowe, *J. Mater. Sci.* **43**, 3960 (2008).

¹⁹C. Wang and C.-Y. Wang, *Surf. Sci.* **602**, 2604 (2008).

²⁰A. G. Evans, D. R. Mumm, J. W. Hutchinson, G. H. Meier, and F. S. Pettit, *Prog. Mater. Sci.* **46**, 505 (2001).

²¹U. Alber, H. Mullejans, and M. Ruhle, *Micron* **30**, 101 (1999).

²²M. C. Munoz, S. Gallego, J. I. Beltran, and J. Cerda, *Surf. Sci. Rep.* **61**, 303 (2006).

²³A. Christensen and E. A. Carter, *J. Chem. Phys.* **114**, 5816 (2001).

²⁴O. I. Malyi, Z. Chen, G. G. Shu, and P. Wu, *J. Mater. Chem.* **21**, 12363 (2011).

²⁵D. J. Siegel, L. G. Hector, Jr., and J. B. Adams, *Phys. Rev. B* **67**, 092105 (2003).

²⁶W. Fu, C. Chang, Y. Chang, C. Yaom, and J. Liao, *Appl. Surf. Sci.* **258**, 8974 (2012).

²⁷H. Zhu, C. Tang, and R. Ramprasad, *Phys. Rev. B* **82**, 235413 (2010).

²⁸H. Zhu and R. Ramprasad, *Phys. Rev. B* **83**, 081416 (2011).

²⁹G. Kresse and J. Furthmuller, *Phys. Rev. B* **54**, 11169 (1996).

³⁰J. P. Perdew, J. A. Chevary, S. H. Vosko, K. A. Jackson, M. R. Pederson, D. J. Singh, and C. Fiolhais, *Phys. Rev. B* **46**, 6671 (1992).

³¹P. E. Blochl, *Phys. Rev. B* **50**, 17953 (1994); G. Kresse and D. Joubert, *ibid.* **59**, 1758 (1999).

³²P. W. Peacock and J. Robertson, *Phys. Rev. Lett.* **92**, 057601 (2004).

³³S. Shi, S. Tanaka, and M. Kohyama, *Phys. Rev. B* **76**, 075431 (2007).

³⁴X. Guo and F. Shang, *Comput. Mater. Sci.* **50**, 1711 (2011).